

Millimeter Wave Automotive Antenna for 5G Communications

Stefano Lenzini^{*(1)}, Agnese Mazzinghi⁽²⁾, Matteo Cerretelli⁽³⁾, and Luca Vincetti⁽¹⁾

(1) Department of Engineering "Enzo Ferrari" (DIEF), University of Modena and Reggio Emilia, 41125 Modena, Italy.

(2) Department of Information Engineering, University of Florence, 50139 Florence, Italy.

(3) ASK Industries S.p.A., 42124 Reggio Emilia, Italy.

Abstract

In this paper an antenna module for automotive 5G communication is presented. The antenna is designed to cover all the 3GPP n258 frequency band i.e. from 24.25 GHz to 27.5 GHz. At these frequencies, the path loss and obstacles attenuation are high. For this reason, to reach an acceptable communication distance a relatively high gain is required. Furthermore, to achieve a more robust system to multipath interferences the antenna is designed to operate with dual linear polarization. The proposed antenna is composed by an array of 8 dual polarized stacked patches. Finally, in order to suppress the radiation pattern distortion due to surface waves (SWs) propagation, an Electronic Band Gap (EBG) structure is implemented. To validate the design a prototype has been realized and measured.

1 Introduction

In recent years, the fast growing of mobile communications demand of throughput and connection reliability, led the allocation of new frequency bands for the mobile standards. In particular, for the 5G in Europe, the so called n258 band (24.25-27.5 GHz) has been allocated in the millimeter wave (mmW) frequency region [1]. The automotive market nowadays requires a full connected vehicle as a mandatory feature. Specific standards have been developed to allow vehicle communications (V2X). The most promising one, primarily thanks to the 5G advent, is based on the mobile network (C-V2X) [2]. The high throughput, high reliable and low latency communications [3][4] allow to use this technology for various applications ranging from the entertainment to the safety ones.

Until now commercial antennas for the automotive market operate up to few GHz [5]-[7] so, the typical installation position on the vehicle is the roof top, where a monopole-like radiation behaviour allows to reach, with a gain ranging from 0 to 5 dBi, all the 360° around the vehicle. At mmWs the attenuation due to obstacles and path loss is higher. For this reason, an antenna with a higher gain is needed to reach acceptable distances. Furthermore, to accomplish the car aesthetic requirements the antenna must be designed with low profile and encumbrance. Printed Circuit Board (PCB) technology is then a valid choice for its low profile and ease

of integration with commercial Monolithic Microwave Integrated Circuits (MMIC).

If an antenna module is placed in each side of the vehicle, in order to reach all the directions, a beamsteering array with steering capability of $\theta = \pm 45^\circ$ on the azimuthal plane is necessary. This concept is illustrated in Fig. 1. On the other hand, on the elevation plane the array should have a beam aperture of at least $\phi = \pm 25^\circ$ in order to deal with the uphill/downhill car travelling conditions. Finally, to have a more robust system to multipath propagation or to exploit polarization diversity in a Multiple Input Multiple Output (MIMO) system a full dual linear polarized antenna should be considered.

In this paper an antenna array suitable for the future 5G automotive applications is presented. The focus of this work is to describe the radiating element design and performances. The antenna achieves a full dual linear polarization operation with a good matching condition in the 5G frequency band from 24.25 to 27.5 GHz. Finally, an EBG structure is exploited to suppress the radiation pattern distortion.

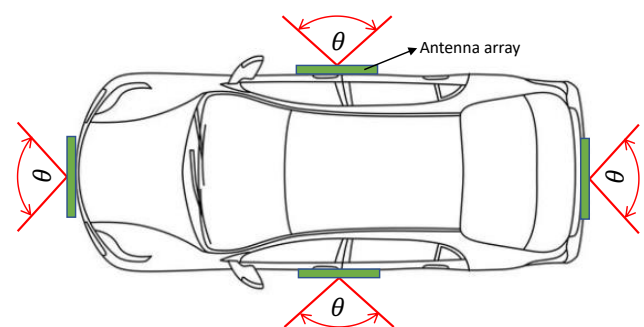


Figure 1. Schematic representation of the mmW antenna modules installation on the car.

2 Antenna Design

2.1 Antenna array

The array is composed by 8 patch antennas placed in a 1x8 configuration as it is illustrated in Fig. 2(a). To reach the desired bandwidth a stacked patch parasitic element is added above the radiating patch. The final stack up is shown in

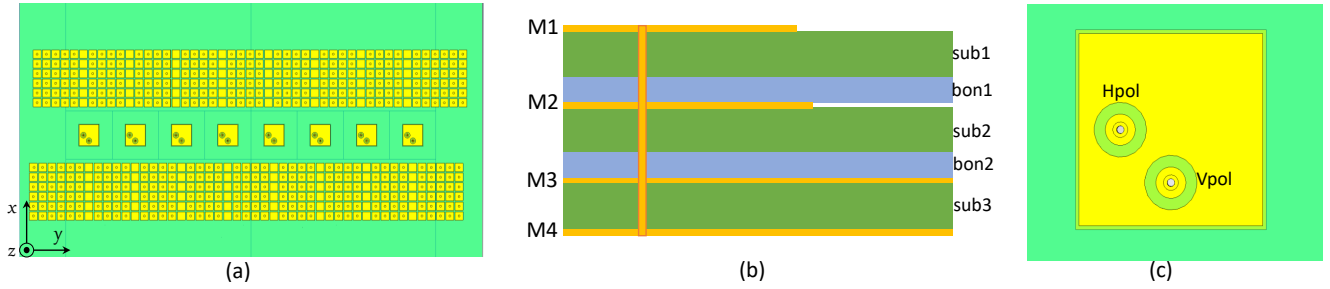


Figure 2. (a) Complete array. (b) PCB stack up, M_n indicates the metal layers, sub_n are the substrate layers while bon_n are the prepreg layers. (c) Detail of the single element.

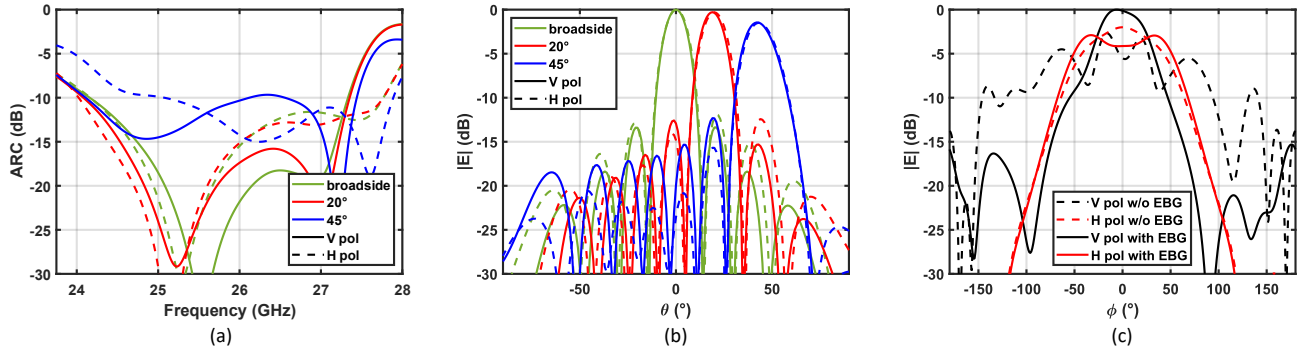


Figure 3. (a) Active Reflection Coefficient of the central element of the array for both the polarizations in 3 different scanning angle configurations. (b) Simulated radiation pattern on the azimuthal plane (θ) for 3 different scanning angles. (c) Simulated radiation pattern cut on the Elevation plane (ϕ) with and without the EBG structure.

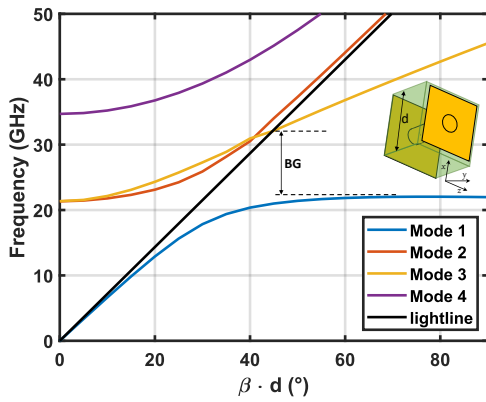


Figure 4. Dispersion diagram of the designed EBG structure. In the inset the simulated unit cell is illustrated. The obtained BG from 22 GHz to 32 GHz is highlighted.

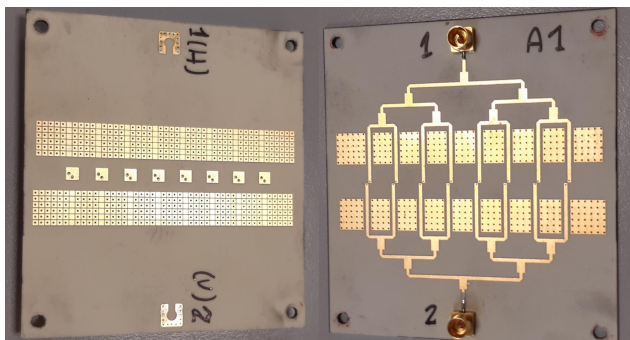


Figure 5. Pictures of the realized prototype. Left side: front view, right side: back view.

Fig. 2(b). The feeding line, realized with microstrips is on metal layer M4, the patch is on M2 and the stacked parasitic element lies on M1. The metal layer M3 act as a ground plane. The feed is realized through a via connecting the microstrips on M4 to the patches on M2. In order to keep the production costs as low as possible only through vias are exploited. For this reason, the feeding vias need to be isolated on the stacked element on layer M1. The isolation can be clearly observed in the single element detail in Fig. 2(c). The radiating patches are designed with a square shape, in this way it is possible to feed them with a 90° mirrored vias to achieve the other linear polarization. Fig. 2(c) highlights the two feeds for the horizontal polarization (H pol) and the vertical polarization (V pol). Simulation [8] results of the Active Reflection Coefficient (ARC) [9] for the centre element of the array is illustrated in Fig. 3(a). The matching is below -10 dB for both the polarizations over the whole n258 band. For a scan angle of 45° the ARC is slightly higher than the -10dB threshold for a small portion of the band but is still acceptable.

2.2 Radiation performances and EBG structure

Simulated radiation patterns at 26GHz for different azimuthal scanning angles ($\theta = zy$ plane) is illustrated in Fig. 3(b). The array achieves 45° of scanning with a Side Lobe Level (SLL) of -12dB. The radiation pattern characteristic on elevation ($\phi = zx$ plane) at 26GHz is drawn in Fig. 3(c). It can be observed that a strong ripple occurs in the vertical

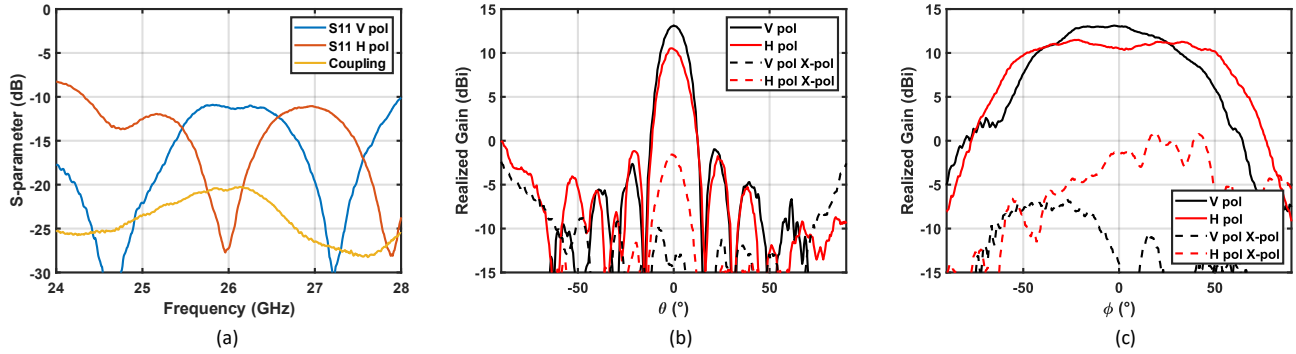


Figure 6. (a) Measured S-parameters of the realized prototype. (b) Measured radiation pattern on the elevation plane (ϕ). (c) Measured radiation pattern on the azimuthal plane (θ).

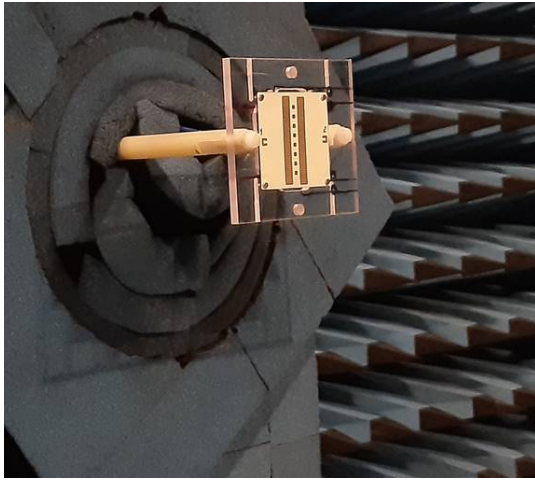


Figure 7. Antenna measurement set-up.

polarization (black dashed lines). To achieve wide bandwidth with patch antennas the substrate needs to be relatively thick respects to the wavelength. This causes a SW to be supported from the substrate [10]. From Fig. 2(a) can be notice that the substrate extends far from the radiating elements along the x direction causing a stronger effect on the vertical polarization respect to the horizontal one.

To mitigate this effect a mushroom-like EBG structure [11] is designed to achieve an operation region where the SW is over cut off for the whole frequency band. EBGs are periodic structures that behaves as a high impedance surface for electromagnetic waves. If correctly designed, it is possible to change the dielectric-air interference conditions creating a forbidden, or Band Gap (BG), frequency region in which the undesired SWs cannot propagate. The mushroom EBG structure is composed by square patches (M1) connected to the ground plane (M3) through a vias, also in this case only through vias are exploited. The unit cell simulated structure, with periodicity d , and the resulting dispersion diagram are illustrated in Fig. 4. The results are obtained with eigenmode solver simulations. Black dashed lines highlight the band gap achieved, that is from 22 to 32 GHz. From black solid line in Fig. 3(c) can be observed how the undesired ripple is mitigated thanks to the EBG. It can be also observed that the achieved gain from the V pol

is now higher than the H pol. This effect occurs because the two regions with the EBG structure act as a wall for the vertical fed patches. Thus, the V pol radiating elements can be considered operating in structure similar to a cavity backed patch antenna [12]. This type of structure is known to increase the gain of the radiating element [13]. However, for both the polarizations the requirement of an elevation aperture grater of $\phi = \pm 25^\circ$ is accomplished

3 Prototype and Measurements Results

To verify the working principle of the antenna the array has been prototyped. The substrates (subn in Fig. 2(b)) are made with Rogers RO4350BLoPro while the bonding layers (bonn in Fig. 2(b)) are Rogers RO4450F. A corporate feed network has been designed to verify the radiation pattern characteristics in the broadside array configuration. The feed is realized through two mini SMP connectors. The prototype is shown in Fig. 5. The measured S-parameters are shown in Fig. 6(a). The antenna achieves a good matching condition (i.e. $S_{11} < -10\text{dB}$) for both the polarization in the whole band while the coupling between the ports remains below -20dB . A picture of the measurement set-up in the anechoic is shown in Fig. 7. The measured azimuthal and elevation planes radiation patterns are shown in Fig. 6(c) an Fig. 6(b) respectively. As expected from simulations the antenna reaches a peak of 13dBi for the V pol and a peak of 11 dBi for the H pol. For both cases, a good polarization purity is achieved, in fact the Cross Polarization (X-pol) level remains below the -10 dB .

4 Conclusion

In this paper a 5G mmW antenna for the automotive market is designed. The whole European 3GPP n258 frequency band is covered with a dual linear polarization operation. Furthermore, an EBG structure is realized to mitigate the SW effects on the radiation patterns. Since the antenna is realized on PCB it is suitable for the integration with commercial MMIC chips in order to realize the desired beam direction.

5 Acknowledgements

This work is supported by the Italian Ministry of Economic Development (MiSE), Innovation Agreements Fund (24th May 2017 decree), position 59, project number F / 130059/00 / X38f.

The authors thanks R. Maggiora and his group at Politecnico di Torino for performing the measurements.

References

- [1] 3GPP TS38.101 [Online]. Available: <https://www.3gpp.org>.
- [2] L. Lusvarghi and M. L. Merani, "On the Coexistence of Aperiodic and Periodic Traffic in Cellular Vehicle-to-Everything," in *IEEE Access*, vol. 8, pp. 207076-207088, 2020, doi: 10.1109/ACCESS.2020.3038307.
- [3] K. Larsson et al., "High-Speed Beam Tracking Demonstrated Using a 28 GHz 5G Trial System," *2017 IEEE 86th Vehicular Technology Conference (VTC-Fall)*, Toronto, ON, 2017, pp. 1-5, doi: 10.1109/VTCFall.2017.8288043.
- [4] J. Mashino, K. Satoh, S. Suyama, Y. Inoue and Y. Okumura, "5G Experimental Trial of 28 GHz Band Super Wideband Transmission Using Beam Tracking in Super High Mobility Environment," *2017 IEEE 85th Vehicular Technology Conference (VTC Spring)*, Sydney, NSW, Australia, 2017, pp. 1-5, doi: 10.1109/VTCSpring.2017.8108644.
- [5] F. Melli, S. Lenzini, M. Cerretelli, E. Coscelli, A. Notari and L. Vincetti, "Low cost 3D tin sheet multi-band shark-fin antenna for LTE MIMO vehicular application," *Microwave and Optical Technology Letters*, 2020, vol. 62, no. 12, pp. 3876– 3880, doi: 10.1002/mop.32493.
- [6] E. Ghafari, A. Fuchs, D. Eblenkamp and D. N. Aloï, "A vehicular rooftop, shark-fin, multi-band antenna for the GPS/LTE/cellular/DSRC systems," *2014 IEEE-APS Topical Conference on Antennas and Propagation in Wireless Communications (APWC)*, Palm Beach, 2014, pp. 237-240, doi: 10.1109/APWC.2014.6905546.
- [7] Y. Liu, Z. Ai, G. Liu and Y. Jia, "An Integrated Shark-Fin Antenna for MIMO-LTE, FM, and GPS Applications," in *IEEE Antennas and Wireless Propagation Letters*, vol. 18, no. 8, pp. 1666-1670, Aug. 2019, doi: 10.1109/LAWP.2019.2927019.
- [8] CST STUDIO SUITE, CST Computer Simulation Technology, 2019.
- [9] D. M. Pozar, "The active element pattern," in *IEEE Transactions on Antennas and Propagation*, vol. 42, no. 8, pp. 1176-1178, Aug. 1994, doi: 10.1109/8.310010.
- [10] D. Pozar and D. Schaubert, "Scan blindness in infinite phased arrays of printed dipoles," in *IEEE Transactions on Antennas and Propagation*, vol. 32, no. 6, pp. 602-610, June 1984, doi: 10.1109/TAP.1984.1143375.
- [11] D. Sievenpiper, Lijun Zhang, R. F. J. Broas, N. G. Alexopolous and E. Yablonovitch, "High-impedance electromagnetic surfaces with a forbidden frequency band," in *IEEE Transactions on Microwave Theory and Techniques*, vol. 47, no. 11, pp. 2059-2074, Nov. 1999, doi: 10.1109/22.798001.
- [12] F. Zavosh and J. T. Aberle, "Single and stacked circular microstrip patch antennas backed by a circular cavity," in *IEEE Transactions on Antennas and Propagation*, vol. 43, no. 7, pp. 746-750, July 1995, doi: 10.1109/8.391152.
- [13] I. Hwang, H. Jo, B. K. Ahn, J. Oh and J. Yu, "Cavity-backed Stacked Patch Array Antenna with Dual Polarization for mmWave 5G Base Stations," *2019 13th European Conference on Antennas and Propagation (EuCAP)*, Krakow, Poland, 2019, pp. 1-5.